

An exact analytic spectrum of relic gravitational waves in an accelerating universe

Y Zhang, X Z Er, T Y Xia, W Zhao and H X Miao

Astrophysics Center, University of Science and Technology of China, Hefei, Anhui, People's Republic of China

E-mail: yzh@ustc.edu.cn

Received 13 September 2005, in final form 27 March 2006

Published 10 May 2006

Online at stacks.iop.org/CQG/23/3783

Abstract

An exact analytic calculation is presented for the spectrum of relic gravitational waves in the scenario of an accelerating universe $\Omega_\Lambda + \Omega_m = 1$. The spectrum formula contains explicitly the parameters of acceleration, inflation, reheating and the tensor/scalar ratio, so that it can be employed for a variety of cosmological models. We find that the spectrum depends on the behaviour of the present accelerating expansion. The amplitude of gravitational waves for the model $\Omega_\Lambda = 0.65$ is about $\sim 50\%$ greater than that of the model $\Omega_\Lambda = 0.7$, an effect accessible to the design sensitivities of LIGO and LISA. The spectrum sensitively depends on inflationary models with $a(\tau) \propto |\tau|^{1+\beta}$, and a larger β yields a flatter spectrum, producing more power. The current LIGO results rule out the inflationary models $\beta \geq -1.8$. LIGO, at its design sensitivity, and LISA will also be able to test the model $\beta = -1.9$. We also examine the constraints on the spectral energy density of relic gravitational waves. Both the LIGO bound and the nucleosynthesis bound rule out the model $\beta = -1.8$, but the model $\beta = -2.0$ is still possible. The exact analytic results also confirm the approximate spectrum and the numerical one from our previous work.

PACS numbers: 98.80.-k, 98.80.Es, 04.30.-w, 04.62.+v

1. Introduction

Recently, much progress has been made in the Laser Interferometer Gravitational waves Observatory (LIGO), with a typical sensitivity of 10^{-22} – 10^{-23} being reached in the frequency range 100–1000 Hz [1–4]. The chance to directly detect gravitational waves (GW) has thus increased. Therefore, it is necessary to examine the possible objects of detections, such as relic GW, which have a spectrum distributed over a rather broad range of frequencies. The stochastic background of relic GW has long been studied [5–7]. The calculation of spectra

generated during a transition from the inflationary era to the radiation-dominated era, or to the matter-dominated era, has been carried out [8–14]. More recently, studies have been made of the detailed slow-roll inflationary effects [15–17], and on the other post-inflationary physical effects on relic GW [18]. A constraint on the tensor-to-scalar ratio r has been derived using the CMB-galaxy cross-correlation [19]. Relic GW can influence the CMB and cause magnetic type CMB polarizations, which can serve as another distinct signal of the relic GW. These kinds of effects have been studied in [20–24]. A recent review of both theoretical and observational issues of the relic GW is given by Grishchuk [25].

The observations of SN Ia [26, 27] indicate that the universe is currently under accelerating expansion, which may be driven by cosmic dark energy ($\Omega_\Lambda \sim 0.7$) plus dark matter ($\Omega_m \sim 0.3$) with $\Omega_\Lambda + \Omega_m = 1$ [28–30]. The evolution of the relic GW after being generated at the inflationary stage depends on the subsequent expansion behaviour of the spacetime background. The current accelerating expansion of the universe will have an impact on the relic GW and their spectrum. The spectrum of the relic GW has been studied in specific models for dark energy, such as the Chaplygin gas model [31] and the X-fluid model [32]. Previously, we have studied the effects on the relic GW caused by the acceleration of the universe for fixed $\Omega_\Lambda = 0.7$ and $\Omega_m = 0.3$, and have obtained an approximate [33], and a numerical spectrum [34] of the relic GW. It was shown that in comparison with the decelerating models, both the shape and amplitude of the spectrum have been modified due to the current accelerating expansion. However, in our previous work, the dependence of the spectrum upon the dark energy fraction Ω_Λ was not examined. Extending these previous studies, in this paper we present an exact analytic calculation of the spectrum for any fraction Ω_Λ of the dark energy. We will demonstrate how Ω_Λ affects the spectrum, and discuss the dependence of the spectrum upon the inflationary models. We will also examine the resulting spectrum by comparing it with the sensitivity curves of the gravitational wave detections, such as LIGO and LISA, and constrain the corresponding spectral energy density by the recent LIGO bound and by the nucleosynthesis bound. The resulting formula of the spectrum will contain explicitly the parameter for dark energy, as well as the parameters for inflationary expansion, reheating, initial normalization of the amplitude and the tensor/scalar ratio, so that it is quite general and can be used in other applications. In this way the paper serves as a useful compilation. Thus, we have listed the main formulae and the relevant specifications involved in the calculation of the spectrum. For convenience throughout the paper we adopt notation similar to that of [10, 33].

2. Expansion stages of the universe

The overall expansion of the spatially flat universe is described by the Robertson–Walker metric $ds^2 = a^2(\tau)[d\tau^2 - \delta_{ij} dx^i dx^j]$, where τ is the conformal time. The scalar factor $a(\tau)$ is given by the following for various stages.

The *initial* stage (inflationary):

$$a(\tau) = l_0 |\tau|^{1+\beta}, \quad -\infty < \tau \leq \tau_1, \quad (1)$$

where $1 + \beta < 0$, and $\tau_1 < 0$. The special case of $\beta = -2$ is the de Sitter expansion of inflation.

The *reheating* stage:

$$a(\tau) = a_z (\tau - \tau_p)^{1+\beta_s}, \quad \tau_1 \leq \tau \leq \tau_s. \quad (2)$$

This stage is introduced to allow a general reheating epoch [10, 33].

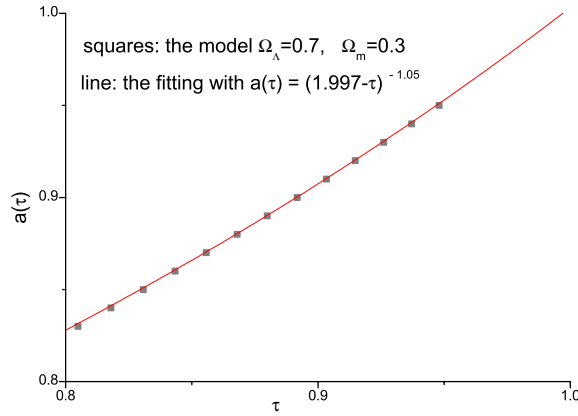


Figure 1. For the accelerating expansion with $\Omega_\Lambda = 0.7$ the scale factor $a(\tau)$ can be fitted by equation (5) with the parameter $\gamma = 1.05$.

The *radiation-dominated* stage:

$$a(\tau) = a_e(\tau - \tau_e), \quad \tau_s \leq \tau \leq \tau_2. \tag{3}$$

The *matter-dominated* stage:

$$a(\tau) = a_m(\tau - \tau_m)^2, \quad \tau_2 \leq \tau \leq \tau_E, \tag{4}$$

where τ_E is the time when the dark energy density ρ_Λ is equal to the matter energy density ρ_m . The redshift z_E at the time τ_E is given by $1 + z_E = \left(\frac{\Omega_\Lambda}{\Omega_m}\right)^{1/3}$. If the current values $\Omega_\Lambda \sim 0.7$ and $\Omega_m \sim 0.3$ are taken, then $1 + z_E \sim 1.33$. For $\Omega_\Lambda \sim 0.65$ and $\Omega_m \sim 0.25$, then $1 + z_E \sim 1.23$ [33].

The *accelerating stage* (up to the present time τ_H):

$$a(\tau) = l_H|\tau - \tau_a|^{-\gamma}, \quad \tau_E \leq \tau \leq \tau_H, \tag{5}$$

where the parameter $\gamma = 1.0$ is the de Sitter acceleration for $\Omega_\Lambda = 1$ and $\Omega_m = 0$. For the realistic model with $\Omega_\Lambda = 0.7$ and $\Omega_m = 0.3$ at present, we have numerically solved the Friedman equation

$$\left(\frac{a'}{a^2}\right)^2 = H^2(\Omega_\Lambda + \Omega_m a^{-3}), \tag{6}$$

where $a' \equiv da(\tau)/d\tau$. The resulting $a(\tau)$ is plotted in figure 1. We have found that the expression of (5) with $\gamma = 1.05$ gives a good fit to the numerical solution $a(\tau)$. Similar calculations show that $\gamma = 1.06$ fits the model $\Omega_\Lambda = 0.65$ (in figure 2), $\gamma = 1.048$ fits the model $\Omega_\Lambda = 0.75$ (in figure 3) and $\gamma = 1.042$ fits the model $\Omega_\Lambda = 0.80$. Thus, for the spatially flat universe ($\Omega_\Lambda + \Omega_m = 1$), as long as the dark energy dominates over the matter component ($\Omega_\Lambda > \Omega_m$), the generic fitting formula (5) is effectively valid, and the range of values for the parameter γ are close to 1.0. The constant τ_a in equation (5) can be taken as the same value, not very sensitive to the various values of Ω_Λ and Ω_m .

There are ten constants in the above expressions of $a(\tau)$, except β , β_s and γ , that are imposed as the model parameters. By the continuity conditions of $a(\tau)$ and $a(\tau)'$ at the four given joining points τ_1 , τ_s , τ_2 and τ_E , one can fix only eight constants. The other two constants can be fixed by the overall normalization of a and by the observed Hubble constant as the expansion rate. Specifically, we put $a(\tau_H) = l_H$ as the normalization, i.e.,

$$|\tau_H - \tau_a| = 1, \tag{7}$$

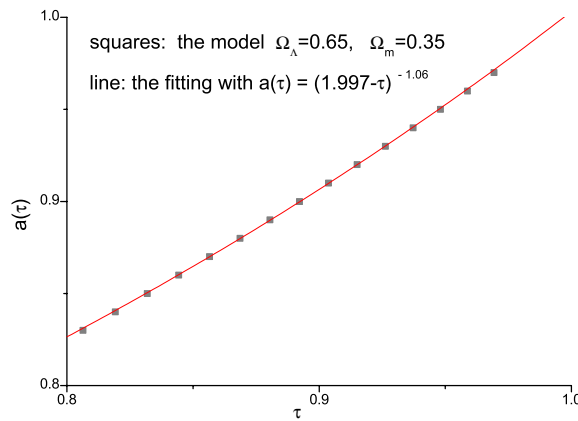


Figure 2. For the accelerating expansion with $\Omega_\Lambda = 0.65$ the scale factor $a(\tau)$ can be fitted by equation (5) with $\gamma = 1.06$.

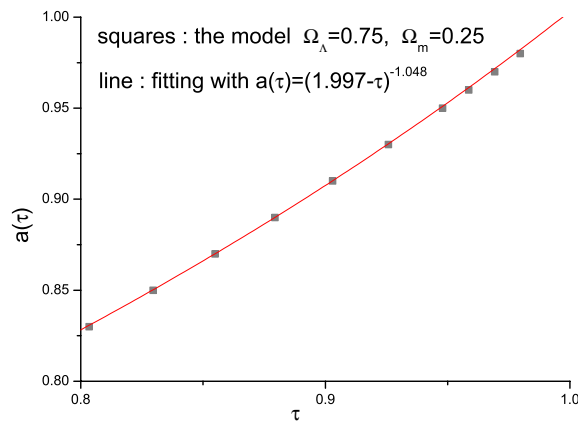


Figure 3. For the accelerating expansion with $\Omega_\Lambda = 0.75$ the scale factor $a(\tau)$ can be fitted by equation (5) with $\gamma = 1.048$.

and the constant l_H is fixed by the following calculation:

$$\frac{1}{H} \equiv \left(\frac{a^2}{a'} \right)_{\tau_H} = \frac{l_H}{\gamma}. \tag{8}$$

As we have shown that $\gamma \simeq 1.0$ in the realistic models of acceleration expansion, so l_H is just the Hubble radius at present. Then everything in the expressions of $a(\tau)$ from equation (1) through to (5) is fixed. For instance, one obtains

$$l_0 = l_H b \gamma \zeta_E^{-(1+\frac{1+\beta}{\gamma})} \zeta_2^{\frac{\beta-1}{2}} \zeta_s^\beta \zeta_1^{\frac{\beta-\beta_s}{1+\beta_s}}, \tag{9}$$

where $b \equiv |1 + \beta|^{-(1+\beta)}$, $\zeta_E \equiv \tau_E/\tau_H$, $\zeta_2 \equiv (\tau_E/\tau_2)^2$, $\zeta_s \equiv \tau_2/\tau_s$ and $\zeta_1 \equiv (\tau_s/\tau_1)^{1+\beta_s}$.

To completely fix the joining conditions we need to specify the time instants τ_1 , τ_2 , τ_s and τ_E that separate two consecutive expansion stages. From the consideration of the physics of the universe, we take the following specifications [33]: $a(\tau_H)/a(\tau_E) = 1.33$,

$a(\tau_E)/a(\tau_2) = 3454$, $a(\tau_2)/a(\tau_s) = 10^{24}$ and $a(\tau_s)/a(\tau_1) = 300$. From these, one makes use of the continuity conditions of a and a' , and obtains

$$\begin{aligned}
 |\tau_E - \tau_a| &= (1 + z_E)^{\frac{1}{\gamma}}, & |\tau_E - \tau_m| &= \frac{2(1 + z_E)}{\gamma}, \\
 |\tau_2 - \tau_m| &= \frac{2(1 + z_E)}{\gamma\sqrt{3454}}, & |\tau_2 - \tau_e| &= \frac{(1 + z_E)}{\gamma\sqrt{3454}}, \\
 |\tau_s - \tau_e| &= \frac{(1 + z_E) \times 10^{-24}}{\gamma\sqrt{3454}}, & |\tau_s - \tau_p| &= (1 + \beta_s) \frac{(1 + z_E) \times 10^{-24}}{\gamma\sqrt{3454}}, \\
 |\tau_1 - \tau_p| &= \frac{(1 + \beta_s) (1 + z_E) \times 10^{-24}}{300^{\frac{1}{\beta_s+1}} \gamma\sqrt{3454}}, & |\tau_1| &= \frac{|1 + \beta| (1 + z_E) \times 10^{-24}}{300^{\frac{1}{\beta_s+1}} \gamma\sqrt{3454}}.
 \end{aligned} \tag{10}$$

The expressions above all depend on the model parameters β , β_s and γ explicitly, and thus depend on Ω_Λ . So we can expect that the spectrum of the relic GW will depend on the present acceleration behaviour of the universe through γ .

In the expanding Robertson–Walker spacetime the physical wavelength λ is related to the comoving wave number k by

$$\lambda \equiv \frac{2\pi a(\tau)}{k}. \tag{11}$$

From equation (7) the wave number corresponding to the present Hubble radius is $k_H = 2\pi a(\tau_H)/l_H = 2\pi$. There is another wave number, $k_E \equiv 2\pi a(\tau_E)H = k_H/(1 + z_E)$, whose corresponding wavelength is the Hubble radius $1/H$ at the time τ_E .

3. The gravitational wave equation

Incorporating the perturbations with the Robertson–Walker metric, one writes

$$ds^2 = a^2(\tau)[d\tau^2 - (\delta_{ij} + h_{ij}) dx^i dx^j], \tag{12}$$

where h_{ij} is 3×3 symmetric, representing the perturbations. The gravitational wave field is the tensorial portion of h_{ij} , which is transverse-traceless $\partial_i h^{ij} = 0$, $\delta^{ij} h_{ij} = 0$, and the wave equation is

$$\partial_\mu (\sqrt{-g} \partial^\mu h_{ij}(\mathbf{x}, \tau)) = 0. \tag{13}$$

For a fixed wave vector \mathbf{k} and a fixed polarization state σ , the wave equation reduces to the second-order ordinary differential equation [33, 35]

$$h_k^{(\sigma)''} + 2\frac{a'}{a}h_k^{(\sigma)'} + k^2 h_k^{(\sigma)} = 0, \tag{14}$$

where the prime denotes $d/d\tau$. Since the equation of $h_{\mathbf{k}}^{(\sigma)}(\tau)$ for each polarization σ is the same, we denote $h_{\mathbf{k}}^{(\sigma)}(\tau)$ by $h_{\mathbf{k}}(\tau)$ in the following. Once the mode function $h_{\mathbf{k}}(\tau)$ is known, the spectrum $h(k, \tau)$ of the relic GW is given by

$$h(k, \tau) = \frac{4l_{pl}}{\sqrt{\pi}} k |h_{\mathbf{k}}(\tau)|, \tag{15}$$

which is defined by the following equation:

$$\int_0^\infty h^2(k, \tau) \frac{dk}{k} \equiv \langle 0 | h^{ij}(\mathbf{x}, \tau) h_{ij}(\mathbf{x}, \tau) | 0 \rangle, \tag{16}$$

where the right-hand side is the vacuum expectation value of the operator $h^{ij}h_{ij}$. The spectral energy density parameter $\Omega_g(k)$ of the GW is defined through the relation

$$\frac{\rho_g}{\rho_c} = \int \Omega_g(k) \frac{dk}{k},$$

where $\rho_g = \frac{1}{32\pi G} h_{ij,0} h_{,0}^{ij}$ is the energy density of the GW, and ρ_c is the critical energy density. Then, one reads

$$\Omega_g(k) = \frac{\pi^2}{3} h^2(k, \tau_H) \left(\frac{k}{k_H} \right)^2, \quad (17)$$

which is dimensionless. Note that there might be divergences in the integration for ρ_g , either infrared or ultraviolet. As is known, the infrared divergence is avoided if an infrared cutoff is introduced. This can be done since the very long waves with wavelengths comparable to, or longer than, the Hubble length do not contribute to the GW energy density [36]. As for the very short wavelength portion, the ultraviolet divergences are also avoided by considering the Parker's adiabatic theorem [37], which states that during a transition between expansion epochs with a characteristic time duration Δt , the gravitons created will be suppressed for wave numbers $k > 1/\Delta t$. Thus, the spectrum segments in both the very low and very high frequency ranges should be discarded from these physical considerations.

4. Initial amplitude of the spectrum

Regarding the relic GW, the initial conditions are taken during the inflationary stage. For a given wave number k , the corresponding wave crosses the horizon at a time τ_i , i.e., when the wavelength is equal to the Hubble radius: $\lambda_i = 2\pi a(\tau_i)/k$ to $1/H(\tau_i)$. Equation (1) yields $H(\tau_i) = l_0^{-1} |1 + \beta| \cdot |\tau_i|^{2+\beta}$, and, for the case of exact de Sitter expansion of $\beta = -2$, one has $H(\tau_i) = l_0^{-1}$. Thus a different k corresponds to a different time τ_i . Now choose the initial condition of the mode function $h_k(\tau)$ as

$$|h_k(\tau_i)| = \frac{1}{a(\tau_i)}. \quad (18)$$

Then the initial amplitude of the spectrum is [10, 33]

$$h(k, \tau_i) = A \left(\frac{k}{k_H} \right)^{2+\beta}, \quad (19)$$

where the constant

$$A = 8\sqrt{\pi} b \frac{l_{Pl}}{l_0}. \quad (20)$$

The power spectrum for the primordial perturbations of energy density is $P(k) \propto |h(k, \tau_H)|^2$, and its spectral index n is defined as $P(k) \propto k^{n-1}$. Thus one reads off the relation $n = 2\beta + 5$. The exact de Sitter expansion of $\beta = -2$ leads to $n = 1$, yielding an initial spectrum independent of k , called the scale-invariant primordial spectrum. Other values of β will differ from the scale-invariant one.

As is known, any calculation of the spectrum of relic GW always has some overall uncertainty, originating from the normalization of the amplitude. Currently, from the observational perspective, the best that one can do is to use the CMB anisotropies to constrain the amplitude, as they receive the contributions from both the scalar (density) and the tensorial (GW) primordial perturbations. However, there is a well-known problem of how much the relative contribution is from the relic GW, in comparison with the scalar-type contribution (the

density perturbations). There have been a number of discussions on the ratio of the relic GW to the scalar contribution,

$$r = P_h/P_s. \tag{21}$$

Theoretically, it is, in our view, a problem of initial conditions on the ratio of the scalar and tensorial modes of cosmic perturbations. So far, in regard to the very long wavelength, some preliminary conclusions on the upper limit of GW contributions have been given, based upon the analysis of WMAP and the observational results of SDSS, for instance, $r < 0.37$ (95% c.l.) [38, 39]. The final conclusion on this issue might eventually rely on more observations of CMB anisotropies and polarization (such as the Planck project in the near future). In the following, the ratio r is treated as a parameter, representing the relative contribution by the relic GW to the CMB anisotropies $\Delta T/T$ at low multipoles. This will determine the overall factor A in (19). Using the observed CMB anisotropies [29] $\Delta T/T \simeq 0.37 \times 10^{-5}$ at $l \sim 2$, which corresponds to anisotropies on the scale of the Hubble radius, we put

$$h(k_H, \tau_H) = 0.37 \times 10^{-5} r. \tag{22}$$

Then the spectrum $h(k, \tau_H)$ at the present time τ_H is fixed. If we take the upper limit $r = 0.37$, then $h(k_H, \tau_H) \simeq 0.14 \times 10^{-5}$. For smaller r , our calculation is still similar except that the resulting spectrum is reduced by the corresponding numerical factor.

5. Analytic solution

Writing the mode function $h_k(\tau) = \mu_k(\tau)/a(\tau)$ in equation (14), the equation for $\mu_k(\tau)$ becomes

$$\mu_k'' + \left(k^2 - \frac{a''}{a}\right) \mu_k = 0. \tag{23}$$

For a scale factor of power-law form $a(\tau) \propto \tau^\alpha$, the general exact solution is of the following form:

$$\mu_k(\tau) = c_1(k\tau)^{\frac{1}{2}} J_{\alpha-\frac{1}{2}}(k\tau) + c_2(k\tau)^{\frac{1}{2}} J_{\frac{1}{2}-\alpha}(k\tau),$$

where the constants c_1 and c_2 are determined by continuity of the function $\mu_k(\tau)$ and the time derivative $(\mu_k(\tau)/a(\tau))'$ at the time instance joining two consecutive stages.

The inflationary stage has the solution

$$\mu_k(\tau) = x^{\frac{1}{2}} [A_1 J_{\beta+\frac{1}{2}}(x) + A_2 J_{-(\beta+\frac{1}{2})}(x)], \quad -\infty < \tau \leq \tau_1, \tag{24}$$

where $x \equiv k\tau$, and the two constants A_1 and A_2 , determining the initial states, are taken to be

$$A_1 = -\frac{i}{\cos \beta\pi} \sqrt{\frac{\pi}{2}} e^{i\pi\beta/2}, \quad A_2 = iA_1 e^{-i\pi\beta}. \tag{25}$$

Both are independent of k . From equation (25) the mode function $\mu_k(\tau)$ is proportional to Hankel's function $H_{\beta+\frac{1}{2}}^{(2)}$,

$$\mu_k(\tau) = A_1 e^{-i\pi\beta} \sin\left(\beta\pi + \frac{\pi}{2}\right) x^{\frac{1}{2}} H_{\beta+\frac{1}{2}}^{(2)}(x), \tag{26}$$

which, in the high frequency limit, approaches the positive frequency mode

$$\lim_{k \rightarrow \infty} \mu_k(\tau) \rightarrow e^{-ik\tau}.$$

Thus the initial state fixed by equation (25) corresponds to the so-called adiabatic vacuum in the high frequency limit [40, 41].

The reheating stage has

$$\mu_k(\tau) = t^{\frac{1}{2}} [B_1 J_{\beta_s+\frac{1}{2}}(t) + B_2 J_{-\beta_s-\frac{1}{2}}(t)], \quad \tau_1 < \tau \leq \tau_s, \quad (27)$$

where the variable $t \equiv k(\tau - \tau_p)$, and the two coefficients B_1 and B_2 are fixed by joining the functions $\mu_k(\tau)$ and $(\mu_k(\tau)/a(\tau))'$ continuously at the time τ_1 when the reheating epoch begins:

$$B_1 = \sqrt{\frac{x_1}{t_1}} \frac{J_{\beta+\frac{1}{2}}(x_1)J_{-\beta_s-\frac{3}{2}}(t_1) + J_{\beta+\frac{3}{2}}(x_1)J_{-\beta_s-\frac{1}{2}}(t_1)}{J_{\beta_s+\frac{1}{2}}(t_1)J_{-\beta_s-\frac{3}{2}}(t_1) + J_{-\beta_s-\frac{1}{2}}(t_1)J_{\beta_s+\frac{3}{2}}(t_1)} A_1 + \sqrt{\frac{x_1}{t_1}} \frac{J_{-\beta-\frac{1}{2}}(x_1)J_{-\beta_s-\frac{3}{2}}(t_1) - J_{-\beta-\frac{3}{2}}(x_1)J_{-\beta_s-\frac{1}{2}}(t_1)}{J_{\beta_s+\frac{1}{2}}(t_1)J_{-\beta_s-\frac{3}{2}}(t_1) + J_{-\beta_s-\frac{1}{2}}(t_1)J_{\beta_s+\frac{3}{2}}(t_1)} A_2, \quad (28)$$

$$B_2 = \sqrt{\frac{x_1}{t_1}} \frac{J_{\beta+\frac{1}{2}}(x_1)J_{\beta_s+\frac{3}{2}}(t_1) - J_{\beta+\frac{3}{2}}(x_1)J_{\beta_s+\frac{1}{2}}(t_1)}{J_{\beta_s+\frac{1}{2}}(t_1)J_{-\beta_s-\frac{3}{2}}(t_1) + J_{-\beta_s-\frac{1}{2}}(t_1)J_{\beta_s+\frac{3}{2}}(t_1)} A_1 + \sqrt{\frac{x_1}{t_1}} \frac{J_{-\beta-\frac{3}{2}}(x_1)J_{\beta_s+\frac{1}{2}}(t_1) + J_{-\beta-\frac{1}{2}}(x_1)J_{\beta_s+\frac{3}{2}}(t_1)}{J_{\beta_s+\frac{1}{2}}(t_1)J_{-\beta_s-\frac{3}{2}}(t_1) + J_{-\beta_s-\frac{1}{2}}(t_1)J_{\beta_s+\frac{3}{2}}(t_1)} A_2 \quad (29)$$

with $x_1 \equiv k\tau_1$, $t_1 \equiv k(\tau_1 - \tau_p)$, and $(1 + \beta_s)x_1 = (1 + \beta)t_1$, which follows from the continuity of $a(\tau)$ and $a'(\tau)$ at the time τ_1 .

The radiation-dominated stage has

$$\mu_k(\tau) = C_1 e^{-iy} + C_2 e^{iy}, \quad \tau_s \leq \tau \leq \tau_2, \quad (30)$$

where the variable $y \equiv k(\tau - \tau_e)$, and C_1 and C_2 are given by

$$C_1 = \frac{e^{iy_s} t_s^{\frac{1}{2}}}{2i} \left\{ \left[\left(i - \frac{1}{y_s} \right) J_{\beta_s+\frac{1}{2}}(t_s) + J_{\beta_s+\frac{3}{2}}(t_s) \right] B_1 + \left[\left(i - \frac{1}{y_s} \right) J_{-\beta_s-\frac{1}{2}}(t_s) - J_{-\beta_s-\frac{3}{2}}(t_s) \right] B_2 \right\}, \quad (31)$$

$$C_2 = \frac{-e^{-iy_s} t_s^{\frac{1}{2}}}{2i} \left\{ \left[- \left(i + \frac{1}{y_s} \right) J_{\beta_s+\frac{1}{2}}(t_s) + J_{\beta_s+\frac{3}{2}}(t_s) \right] B_1 + \left[- \left(i + \frac{1}{y_s} \right) J_{-\beta_s-\frac{1}{2}}(t_s) - J_{-\beta_s-\frac{3}{2}}(t_s) \right] B_2 \right\}, \quad (32)$$

where $t_s \equiv k(\tau_s - \tau_p)$, $y_s \equiv k(\tau_s - \tau_e)$ and $t_s = (1 + \beta_s)y_s$.

The matter-dominated stage has

$$\mu_k(\tau) = \sqrt{\frac{\pi z}{2}} [D_1 J_{\frac{3}{2}}(z) + D_2 J_{-\frac{3}{2}}(z)], \quad \tau_2 \leq \tau \leq \tau_E, \quad (33)$$

where $z \equiv k(\tau - \tau_m)$, and D_1 and D_2 are given by

$$D_1 = \left[-e^{iy_2} - \frac{i}{2y_2} e^{iy_2} + \frac{e^{iy_2} + e^{-3iy_2}}{8y_2^2} \right] C_1 + \left[-e^{-iy_2} + \frac{i}{2y_2} e^{-iy_2} + \frac{e^{-iy_2} + e^{3iy_2}}{8y_2^2} \right] C_2, \quad (34)$$

$$D_2 = \left[ie^{iy_2} - \frac{e^{iy_2}}{2y_2} - \frac{i}{8y_2^2} (e^{iy_2} - e^{-3iy_2}) \right] C_1 - \left[ie^{-iy_2} + \frac{e^{-iy_2}}{2y_2} + \frac{i}{8y_2^2} (e^{3iy_2} - e^{-iy_2}) \right] C_2, \quad (35)$$

with $y_2 \equiv k(\tau_2 - \tau_e)$.

The accelerating stage has

$$\mu_k(\tau) = \sqrt{\frac{\pi s}{2}} [E_1 J_{\gamma+\frac{1}{2}}(s) + E_2 J_{-\gamma-\frac{1}{2}}(s)], \quad \tau_E \leq \tau \leq \tau_H, \quad (36)$$

where $s \equiv k(\tau - \tau_a)$, and E_1 and E_2 are given by

$$E_1 = \Delta^{-1} \frac{z_E}{s_E} \left\{ J_{\frac{3}{2}}(z_E) \left[-\frac{J_{-\gamma-\frac{1}{2}}(s_E)}{s_E} - J_{-\gamma-\frac{3}{2}}(s_E) \right] - J_{\frac{5}{2}}(z_E) J_{-\gamma-\frac{1}{2}}(s_E) \right\} D_1 + \left\{ J_{-\frac{3}{2}}(z_E) \left[-\frac{J_{-\gamma-\frac{1}{2}}(s_E)}{s_E} - J_{-\gamma-\frac{3}{2}}(s_E) \right] + J_{-\frac{5}{2}}(z_E) J_{-\gamma-\frac{1}{2}}(s_E) \right\} D_2, \quad (37)$$

$$E_2 = \Delta^{-1} \frac{z_E}{s_E} \left\{ J_{\frac{3}{2}}(z_E) J_{\gamma+\frac{1}{2}}(s_E) - J_{\frac{3}{2}} \left[-\frac{J_{\gamma+\frac{1}{2}}(s_E)}{s_E} + J_{\gamma+\frac{3}{2}}(s_E) \right] \right\} D_1 + \left\{ -J_{-\frac{5}{2}}(z_E) J_{\gamma+\frac{1}{2}}(s_E) - J_{-\frac{3}{2}} \left[-\frac{J_{\gamma+\frac{1}{2}}(s_E)}{s_E} + J_{\gamma+\frac{3}{2}}(s_E) \right] \right\} D_2. \quad (38)$$

$$\Delta = J_{\gamma+\frac{1}{2}}(s_E) \left[-\frac{J_{-\gamma-\frac{1}{2}}(s_E)}{s_E} - J_{-\gamma-\frac{3}{2}}(s_E) \right] - J_{-\gamma-\frac{1}{2}}(s_E) \left[-\frac{J_{\gamma+\frac{1}{2}}(s_E)}{s_E} + J_{\gamma+\frac{3}{2}}(s_E) \right] \quad (39)$$

where $z_E \equiv k(\tau_E - \tau_m)$, $s_E \equiv k(\tau_E - \tau_a)$ and $\gamma z_E = -2s_E$.

With all these coefficients having been fixed, the mode function $h_k(\tau_H)$ is known as a function of the wave number k at present time τ_H , so is the spectrum

$$h(k, \tau_H) = \frac{4l_{Pl}}{\sqrt{\pi}} k |h_k(\tau_H)|, \quad (40)$$

as defined in equation (15). The above results form a useful compilation for computing the relic GW. To make use of formulation (40), one substitutes $h_k(\tau_H) = \mu_k(\tau_H)/a(\tau_H)$, where $\mu_k(\tau_H)$ is given in equation (36). Of course, to specify $\mu_k(\tau_H)$, all the coefficients E_1, E_2 throughout A_1, A_2 have to be employed. One may, in his own computation, choose proper values of the parameters β, β_s and γ for the specific expansion behaviour, as well as the initial amplitude A in equation (22).

For illustrations, taking the tensor/scalar ratio in equation (21) $r = 0.37$, we have plotted the exact spectrum $h(k, \tau_H)$ as a function of the frequency $\nu = k/2\pi a$ in figure 4 for $\gamma = 1.05$ and in figure 5 for $\gamma = 1.06$. In each of these figures of fixed γ , three spectra are shown for three inflationary models with $\beta = -1.8, -1.9$ and -2.0 , and $\beta_s = 0.598, -0.552$ and -0.689 , respectively [33]. As these figures show, the spectrum is scale invariant with a flat segment in the range $\nu \leq 10^{-18}$ Hz and a slope segment in the range $\nu \geq 10^{-18}$ Hz.

Now we make a comparison of the exact spectrum $h(\nu, \tau_H)$ with the sensitivity curve from the recent S2 of LIGO [1, 2, 4] with a sensitivity of 10^{-22} to 10^{-23} in the frequency range $\nu = 10^2 \sim 10^3$ Hz. $h(\nu, \tau_H)$ is given in figure 6 for $\gamma = 1.05$ and in figure 7 for $\gamma = 1.06$. Both figures have three spectra plotted for inflationary models $\beta = -1.8, \beta = -1.9$ and $\beta = -2.0$, respectively. It is found that the inflationary models with $\beta \geq -1.8$ have an amplitude about an order higher than the LIGO sensitivity curve. Even if we take a much lower value for the tensor/scalar ratio, say $r = 0.05$, the spectrum is still within the region detectable by LIGO. Thus, the inflationary model $\beta = -1.8$ generating relic GW with $r > 0.05$ is ruled out by the LIGO null results. The models $\beta \leq -1.9$ are still possible by this test alone. Moreover, when LIGO reaches its design sensitivity $\sim 10^{-24}$ in the frequency range in forthcoming runs, it will also be able to test the model $\beta = -1.9$.

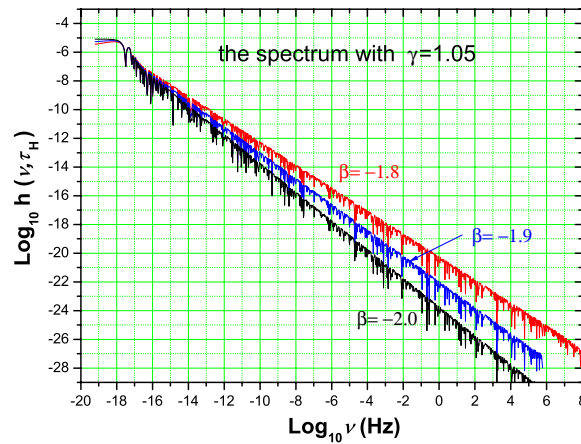


Figure 4. For a fixed acceleration parameter $\gamma = 1.05$ the exact spectrum $h(\nu, \tau_H)$ is plotted for three inflationary models, $\beta = -1.8$, $\beta = -1.9$ and $\beta = -2.0$, respectively.

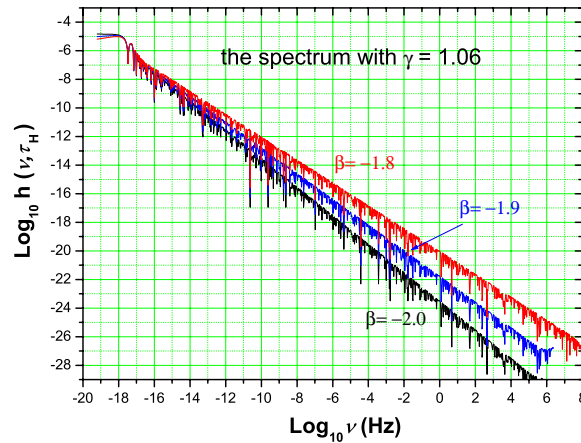


Figure 5. For a fixed acceleration parameter $\gamma = 1.06$ the exact spectrum $h(\nu, \tau_H)$ is plotted for three inflationary models, $\beta = -1.8$, $\beta = -1.9$ and $\beta = -2.0$, respectively.

Figure 8 for $\gamma = 1.05$ and figure 9 for $\gamma = 1.06$ give a comparison of the exact spectra $h(\nu, \tau_H)$ with the sensitivity curve from the next generation LISA [42] in the lower frequency range $\nu = 10^{-4}$ – 10^2 Hz. It is interesting to note that when LISA, as being designed, runs in space in the near future, it will be able to examine directly not only the model $\beta = -1.8$ but also the model $\beta = -1.9$. For the latter model, even if a much lower value of the ratio $r = 0.05$ is taken, LISA will still be able to detect it. This will be an improvement on the LIGO detection on Earth. However, as the two figures show, the inflationary model $\beta = -2.0$ seems to be still difficult to detect by LISA as presently designed.

Let us examine the dependence of the spectrum $h(\nu, \tau_H)$ upon the dark energy Ω_Λ through the acceleration model parameter γ . In figure 10, for a fixed $\beta = -2.0$ we plot two spectra $h(\nu, \tau_H)$ for the acceleration models $\gamma = 1.05$ and $\gamma = 1.06$ in a broad range of frequencies. As is seen, the difference between these two acceleration models is small. To show the details

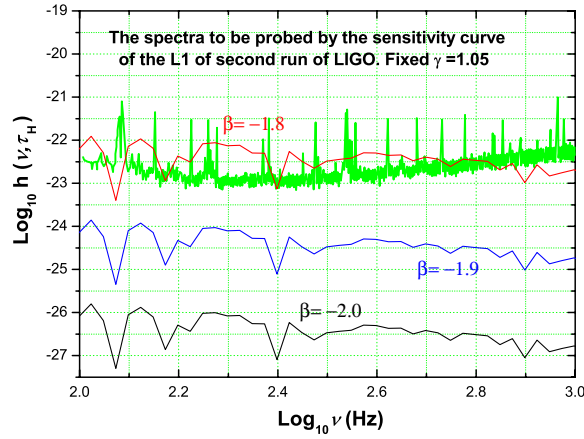


Figure 6. For a fixed acceleration parameter $\gamma = 1.05$ the exact spectrum $h(\nu, \tau_H)$ is plotted within the range of $\nu = 10^2$ – 10^3 Hz for three inflationary models, $\beta = -1.8$, $\beta = -1.9$ and $\beta = -2.0$, to compare with the sensitivity curve of second run of LIGO L1 [4].

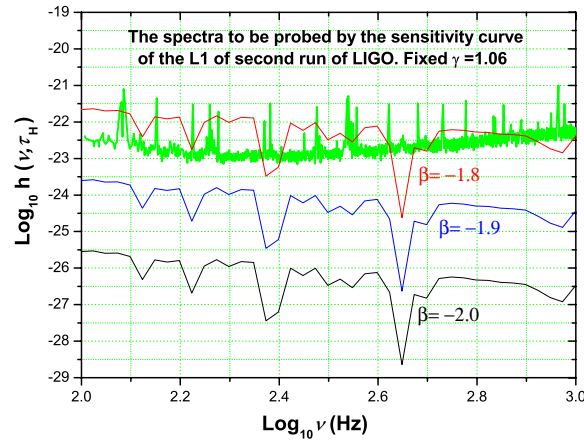


Figure 7. For a fixed acceleration parameter $\gamma = 1.06$ the exact spectrum $h(\nu, \tau_H)$ is plotted within the range of $\nu = 10^2$ – 10^3 Hz for three inflationary models, $\beta = -1.8$, $\beta = -1.9$ and $\beta = -2.0$, to compare with the sensitivity curve of second run of LIGO L1 [4].

as enlarged pictures, in figures 11 and 12 we have plotted the spectra over a narrow range of frequencies. It can be read that the amplitude of the model $\gamma = 1.06$ is about $\sim 50\%$ greater than that of the model $\gamma = 1.05$. That is, in the accelerating universe with $\Omega_\Lambda = 0.65$ the amplitude of the relic GW is $\sim 50\%$ higher than the one with $\Omega_\Lambda = 0.7$. Note that the spectrum amplitude $h(\nu, \tau_H)$ itself is very small, so this difference of $\sim 50\%$ is probably difficult to detect at present. However, in principle, it does provide a new way of revealing the dark energy fraction Ω_Λ in the universe. With LIGO approaching its design sensitivity, this difference will hopefully be detected. As LISA is currently designed, it will also be able to detect this effect.

Let us examine the spectral energy densities $\Omega_g(\nu)$ and their constraints. Figures 13 and 14 are the plots of the spectral energy density $\Omega_g(\nu)$ defined in equation (17) for $\gamma = 1.05$

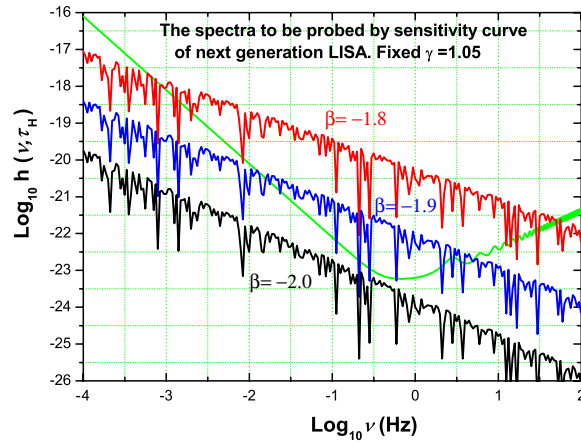


Figure 8. For a fixed acceleration parameter $\gamma = 1.05$ the exact spectrum $h(\nu, \tau_H)$ is plotted within the range of $\nu = 10^{-4}$ – 10^2 Hz for three inflationary models, $\beta = -1.8$, $\beta = -1.9$ and $\beta = -2.0$, to compare with the sensitivity of the next generation LISA [42].

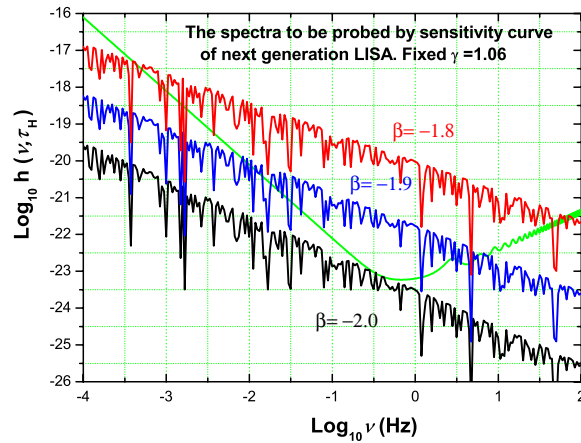


Figure 9. For a fixed acceleration parameter $\gamma = 1.06$ the exact spectrum $h(\nu, \tau_H)$ is plotted within the range of $\nu = 10^{-4}$ – 10^2 Hz for three inflationary models, $\beta = -1.8$, $\beta = -1.9$ and $\beta = -2.0$, to compare with the sensitivity of the next generation LISA [42].

and $\gamma = 1.06$, respectively. These plots of the exact analytic results agree with the numerical one in [34]. If we use the result of the LIGO third science run [3] for the energy density bound for the flat spectrum with $\Omega_0 < 8.4 \times 10^{-4}$ in the 69–156 Hz band, then the model $\beta = -1.8$ is ruled out, but the models $\beta \leq -1.9$ survive. However, this LIGO constraint on the GW energy density is not as stringent as the constraint by the so-called nucleosynthesis bound [43, 44], the idea of which is as follows. In the early universe at a temperature $T \sim$ a few MeV the nucleosynthesis process goes on. The relic GW will contribute to the total energy density ρ that drives the universe expansion, and thus will increase the effective number of species of particles g_* . More relic GW energy will enhance the freeze-out temperature for the process $pe \leftrightarrow n\nu$, and will lead to more neutrons being available for the production of

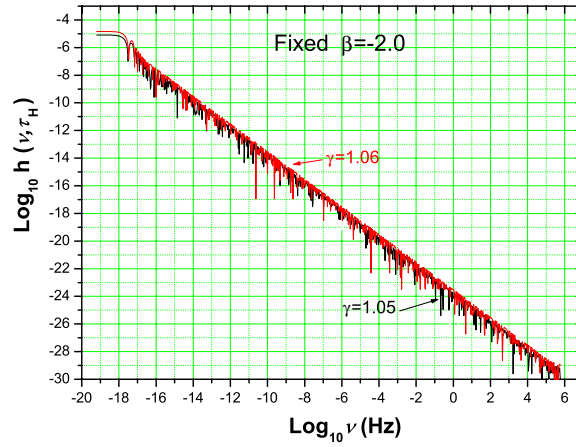


Figure 10. For a fixed inflationary parameter $\beta = -2.0$ the spectrum $h(v, \tau_H)$ is plotted for different acceleration models, $\gamma = 1.05$ and $\gamma = 1.06$. The two spectra are quite close to each other, and the difference in amplitudes of $h(v, \tau_H)$ is quite small, and difficult to tell from this figure.

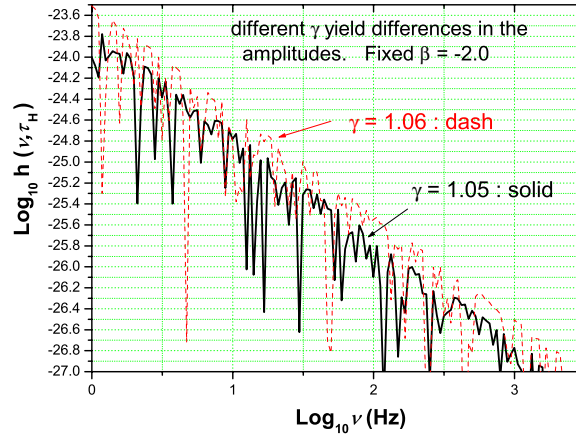


Figure 11. This enlargement is a portion of figure 10 in the range $\nu = 1-10^3$ Hz to show the differences in the spectrum $h(v, \tau_H)$ for different acceleration models. Note that the amplitude of $h(v, \tau_H)$ for the model $\gamma = 1.06$ is about $\sim 50\%$ higher than that of model $\gamma = 1.05$. But in the range $\nu = 10^2-10^3$ Hz the amplitude is only about $\leq 3 \times 10^{-26}$, which is not yet accessible to the current LIGO.

helium-4 (${}^4\text{He}$). In practice, the effective number of neutrino species N_ν is used in place of g_* . The analysis has led to the nucleosynthesis bound on the relic GW energy density at the present time [43],

$$\int \Omega_g(\nu) d(\log \nu) \leq 0.56 \times 10^{-5}, \quad (41)$$

where the value $\rho_\gamma \simeq 2.481 \times 10^{-5} \rho_c$ and a conservative value of $N_\nu < 4$ have been used. Note that this is bound on the total GW energy density integrated over all frequencies. The integrand function should also have a bound $\Omega_g(\nu) < 0.56 \times 10^{-5}$ in the interval of

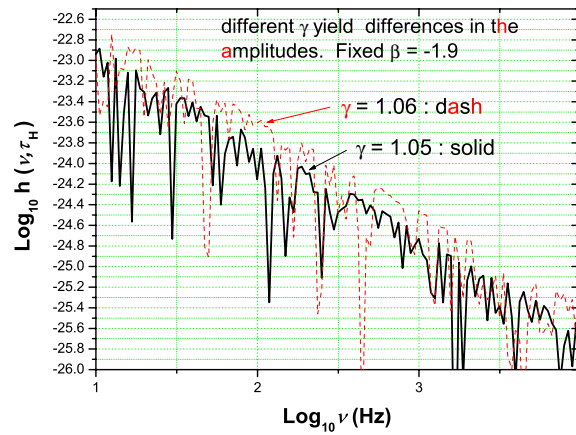


Figure 12. For fixed $\beta = -1.9$ this enlargement in the range $\nu = 10\text{--}10^4$ Hz shows the differences in the spectrum $h(\nu, \tau_H)$ for different acceleration models. Again the amplitude of $h(\nu, \tau_H)$ for the model $\gamma = 1.06$ is about $\sim 50\%$ higher than that of model $\gamma = 1.05$. Now in the range $\nu = 10^2 - 3 \times 10^2$ Hz the amplitude is about $\sim 10^{-24}$, accessible to LIGO as it approaches its design sensitivity of 10^{-24} .

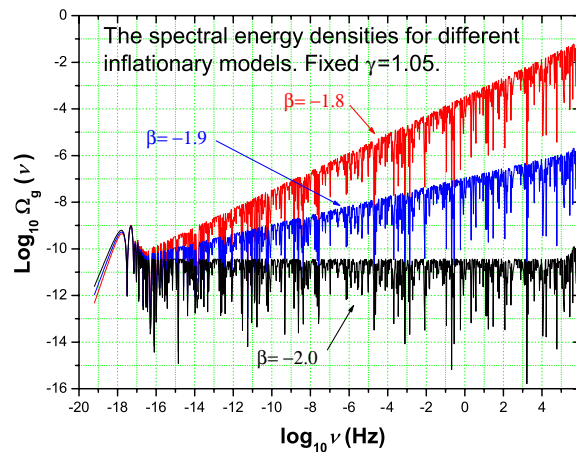


Figure 13. For fixed $\gamma = 1.05$ the spectral energy density $\Omega_g(\nu)$ is plotted for the models $\beta = -1.8$, $\beta = -1.9$ and $\beta = -2.0$. Obviously, the inflationary model $\beta = -1.8$ has an $\Omega_g(\nu)$ increasing too rapidly with the frequency ν , and is thus ruled out by the LIGO bound and the nucleosynthesis bound. $\Omega_g(\nu)$ in the model $\beta = -1.9$ is narrowly below the nucleosynthesis bound but since $\Omega_g(\nu)$ also increases too rapidly with ν so it will barely survive. The model of $\beta = -2.0$ has a flat spectral energy density with a value $\sim 10^{-10}$, much lower than the nucleosynthesis bound. Thus the model $\beta = -2.0$ is robust.

frequencies $\delta(\log \nu) \simeq 1$. By this constraint it is also seen from figures 13 and 14 that the model $\beta = -1.8$ has an $\Omega_g(\nu)$ that is too high and therefore ruled out, the same conclusion that we arrived at from figures 6 and 7. The model with $\beta = -1.9$ is barely possible, as its energy density $\Omega_g(\nu)$ tends to grow higher with high frequencies. The model $\beta = -2.0$ is still robust since its spectral energy density $\Omega_g(\nu)$ is a flat function much lower than the limit in equation (41).

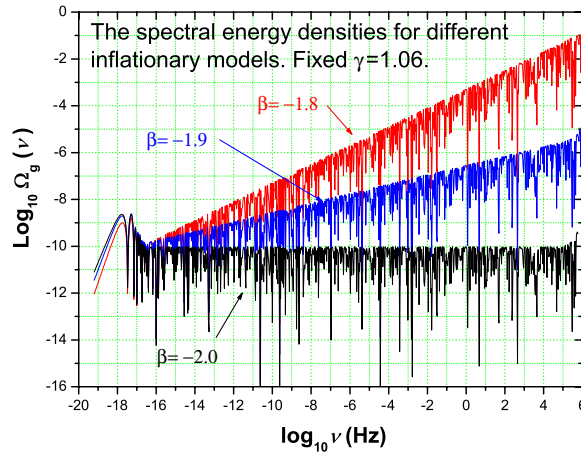


Figure 14. This figure is similar to figure 13 but for fixed $\gamma = 1.06$. The conclusions are also similar to those from figure 13.

6. Analytic approximation

We now give an approximation to the above exact solution $h(k, \tau_H)$ to recover the approximate analytic one given in [33]. The following approximation for the Bessel functions will be used:

$$J_\mu(x) \approx \sqrt{\frac{2}{\pi x}} \cos\left(x - \frac{\mu\pi}{2} - \frac{\pi}{4}\right), \quad x \gg 1, \tag{42}$$

$$J_\mu(x) \approx \frac{1}{\Gamma(\mu + 1)} \left(\frac{x}{2}\right)^\mu, \quad x \ll 1. \tag{43}$$

Note that the coefficients $D_1, D_2, B_1, B_2, C_1, C_2, E_1$ and E_2 are all functions of k , and they need to be approximated according to the value of k .

In the long-wave limit, $x_1 = k\tau_1 \ll 1$ and $t_1 = (1 + \beta_s)x_1 / (1 + \beta) \ll 1$, from equations (28) and (29) one has

$$D_1 \approx 2^{-\beta + \beta_s} \left(\frac{1 + \beta}{1 + \beta_s}\right)^{\beta + 1} t_1^{\beta - \beta_s} A_1, \quad D_2 \approx t_1^{\beta + \beta_s + 3} A_1. \tag{44}$$

D_2 is a higher order of t_1 and can be neglected in the following.

From equations (31) and (32), in the long-wave limit $t_s \ll 1$ and $y_s \ll 1$, one has

$$B_1 \approx i t_s^{\beta_s} D_1 \propto k^\beta, \quad B_2 \approx -B_1. \tag{45}$$

From equations (34) and (35), in the long-wave limit $k \ll 1/\tau_2$, one has

$$C_1 \approx -\frac{3i}{2y_2} B_1 \sim k^{\beta - 1}, \quad C_2 \ll C_1, \tag{46}$$

so C_2 can be neglected. In the short-wave limit $k \gg 1/\tau_2$, one has

$$C_1 \approx -2iB_1 \sin z_2, \quad C_2 \approx 2iB_1 \cos z_2. \tag{47}$$

From equations (37) and (38), for $k\tau_E \ll 1$, one has

$$E_1 \approx C_1, \quad E_2 \approx C_2, \tag{48}$$

which also holds approximately for $k\tau_E \gg 1$, with some extra oscillating factors.

With all these coefficients being estimated, we can now evaluate the approximation of the spectrum in equation (15) at the present time τ_H , which is written as

$$h(k, \tau_H) = A \frac{l_0}{2\pi b} k \left| \frac{\mu_k(\tau_H)}{a(\tau_H)} \right|.$$

Substituting expressions (36) for $\mu_k(\tau_H)$ and equation (9) for l_0 into the above leads to

$$h(k, \tau_H) = A \left[\gamma (\zeta_E)^{-(1+\frac{1+\beta}{\gamma})} \zeta_2^{\frac{\beta-1}{2}} \zeta_s^\beta \zeta_1^{\frac{\beta_s-\beta}{1+\beta_s}} \right] \frac{k}{k_H} \sqrt{\frac{\pi s_H}{2}} |E_1 J_{\gamma+\frac{1}{2}}(s_H) + E_2 J_{-\gamma-\frac{1}{2}}(s_H)|. \quad (49)$$

Using the results from equations (42) through to (48), we approximate this expression by the leading term of the power-law of k in various ranges of k . By some straightforward calculations, using $|(\tau_H - \tau_a)/(\tau_E - \tau_2)| = 1/(1+z_E)$, we obtain the following expressions for the analytic approximate spectrum:

$$h(k, \tau_H) = A \left(\frac{k}{k_H} \right)^{2+\beta}, \quad k \leq k_E; \quad (50)$$

$$h(k, \tau_H) \approx A \left(\frac{k}{k_H} \right)^{\beta-1} \frac{1}{(1+z_E)^{3+\epsilon}}, \quad k_E \leq k \leq k_H; \quad (51)$$

$$h(k, \tau_H) \approx A \left(\frac{k}{k_H} \right)^\beta \frac{1}{(1+z_E)^{3+\epsilon}}, \quad k_H \leq k \leq k_2; \quad (52)$$

$$h(k, \tau_H) \approx A \left(\frac{k}{k_H} \right)^{\beta+1} \frac{k_H}{k_2} \frac{1}{(1+z_E)^{3+\epsilon}}, \quad k_2 \leq k \leq k_s; \quad (53)$$

$$h(k, \tau_H) \approx A \left(\frac{k_s}{k_H} \right)^{\beta_s} \frac{k_H}{k_2} \left(\frac{k}{k_H} \right)^{\beta-\beta_s+1} \frac{1}{(1+z_E)^{3+\epsilon}}, \quad k_s \leq k \leq k_1, \quad (54)$$

where the small parameter $\epsilon \equiv (1+\beta)(1-\gamma)/\gamma$, also depending on the behaviour of the acceleration expansion through γ . The model $\gamma = 1$ gives $\epsilon = 0$, and the results of equations (50) through to (54) reduce to exactly our early result given in [33]. The influence of the detailed accelerating expansion on the $h(k, \tau_H)$ is mainly demonstrated through the factor $1/(1+z_E)^{3+\epsilon}$, causing a variation in the magnitude of $h(k, \tau_H)$. For the inflationary expansion with $\beta \approx -2$, the model $\gamma = 1.05$ ($\Omega_\Lambda = 0.7$) gives $1/(1+z_E)^{3+\epsilon} = 0.423$, and the model $\gamma = 1.06$ ($\Omega_\Lambda = 0.65$) gives $1/(1+z_E)^{3+\epsilon} = 0.533$, yielding an amplitude of the model $\gamma = 1.06$ that is greater than that of the model $\gamma = 1.05$ by about $\sim 30\%$. The more accurate computation from the exact solutions shows an average difference of $\sim 50\%$, as plotted in figures 11 and 12. Note that the factor $1/(1+z_E)^\epsilon = 0.987$ for the model $\gamma = 1.05$, and $1/(1+z_E)^\epsilon = 0.989$ for the model $\gamma = 1.06$, differs by only 0.2% , which is too small to detect by the current experimental detectors. Therefore, with regard to the amplitude of the relic GW, one can simply put $\epsilon = 0$ in the approximate spectrum given in equations (50)–(54), just as it was in the model $\gamma = 1$, causing only a difference of 0.2% in the amplitude for a variety of models with various γ .

We remark that each of these expressions from equations (51) to (54) holds up to a numerical factor A , which contains certain oscillating factors of the form $\cos(k\tau_H)$, or $\cos(y_2)$ and $\sin(t_s)$. In comparison with the decelerating models [10], equation (51) is a new segment of spectrum in $k_E < k < k_H$, whose occurrence is due to the acceleration of the current expansion of the universe. Besides, the three segments of the spectrum, i.e., equations (52)–(54), all have the extra factor $(1+z_E)^{-3-\epsilon} = (\Omega_m/\Omega_\Lambda)^{1+\epsilon/3}$ that is missing in the corresponding three segments in the decelerating models.

7. Conclusion

We have presented a detailed calculation of the exact analytic spectrum of relic GW in the present flat $\Omega_\Lambda + \Omega_m = 1$ universe in accelerating expansion. The resulting exact spectrum explicitly depends on the detailed behaviour of the present accelerating expansion, characterized by the parameter γ in the scale factor $a(\tau) \propto |\tau|^{-\gamma}$. It also explicitly depends on the inflationary model β , the reheating model β_s and the tensor/scalar ratio r as well. Therefore, the result is general enough to describe the GW spectrum $h(\nu, \tau_H)$ produced from a variety of accelerating cosmological models. One can use the formula in other applications by choosing a set of parameters β , β_s , γ and r . Besides, the analysis of the exact result gives the following conclusions.

The GW amplitude of the model $\gamma = 1.06$ is about $\sim 50\%$ greater than that of the model $\gamma = 1.05$, i.e., in the accelerating universe with $\Omega_\Lambda = 0.65$, the amplitude of the relic GW is $\sim 50\%$ higher than the one with $\Omega_\Lambda = 0.7$. Although it is probably difficult to detect at present, the effect does provide a new way to identify the dark energy fraction Ω_Λ in the universe. Hopefully this difference can be detected when LIGO approaches its design sensitivity of $\sim 10^{-24}$, and in LISA runs in the future.

The spectrum is sensitive to the parameter β of the inflationary model. A larger value of β yields a flatter spectrum $h(\nu, \tau_H)$ with more power on the higher frequencies. The sensitivity curve of the current LIGO rules out inflationary models with $\beta \geq -1.8$. LIGO at its design sensitivity and LISA in future will also be able to test the $\beta = -1.9$ model directly.

The relic GW are also constrained through their spectral energy density $\Omega_g(\nu)$ by the recent LIGO bound and the nucleosynthesis bound. While both bounds rule out the inflationary model $\beta = -1.8$, the nucleosynthesis bound puts the model $\beta = -1.9$ in danger. However, the model $\beta = -2.0$ (de Sitter) is robust, since its spectral energy density $\Omega_g(\nu)$ is flat and is $\sim 10^{-10}$, much lower than the nucleosynthesis bound.

Finally, the exact analytic spectrum reduces to the approximate analytic and the numerical ones given in our previous study for the case $\gamma = 1$.

Acknowledgments

YZ's research work was supported by the Chinese NSF (10173008), NKBRSF (G19990754) and by SRFDP.

References

- [1] Abbott R *et al* 2005 *Phys. Rev. D* **72** 062001 (Preprint gr-qc/0505029)
- [2] Abbott R 2005 *Phys. Rev. Lett.* **94** 181103
- [3] Abbott B *et al* 2005 *Phys. Rev. Lett.* **95** 221101 (Preprint gr-qc/0507254)
- [4] Abbott B *et al* 2005 *Phys. Rev. D* **72** 102004 (Preprint gr-qc/0508065)
- [5] Starobinsky A A 1979 *JETP Lett.* **30** 682
- [6] Rubakov V A, Sazhin M V and Veryaskin A V 1982 *Phys. Lett. B* **115** 189
- [7] Abbott L F and Harari D D 1986 *Nucl. Phys. B* **264** 487
- [8] Allen B 1988 *Phys. Rev. D* **37** 2078
- [9] Sahni V 1990 *Phys. Rev. D* **42** 453
- [10] Grishchuk L 1997 *Class. Quantum Grav.* **14** 1445
Grishchuk L 2001 *Lecture Notes in Physics* vol 562 (Berlin: Springer) p 164
Grishchuk L 2001 *Gyros, Clocks, Interferometers . . . : Testing Relativistic Gravity in Space* ed C Lammerzahl *et al* (Berlin: Springer)
- [11] Maia M R G and Barrow J D 1994 *Phys. Rev. D* **50** 6262
- [12] Riszuelo A and Uzan J-P 2000 *Phys. Rev. D* **62** 083506

- [13] Tashiro H, Chiba K and Sasaki M 2004 *Class. Quantum Grav.* **21** 1761
- [14] Henriques A B 2004 *Class. Quantum Grav.* **21** 3057
Henriques A B and Mendes L M 1995 *Phys. Rev. D* **52** 2083
- [15] Gong G 2004 *Class. Quantum Grav.* **21** 5555–62
- [16] Ungarelli C *et al* 2005 *Class. Quantum Grav.* **22** S955–64
- [17] Smith T L, Kamionkowski M and Cooray A 2005 *Preprint astro-ph/0506422*
- [18] Boyle L B and Steinhardt P J 2005 *Preprint astro-ph/0512014*
- [19] Cooray A *et al* 2005 *Phys. Rev. D* **72** 023514
- [20] Hu W and White M 1997 *Phys. Rev. D* **56** 597
- [21] Zaldarriaga M and Harari D D 1995 *Phys. Rev. D* **52** 3276
Harari D and Zaldarriaga M 1993 *Phys. Lett. B* **310** 96
- [22] Kamionkowski M, Kosowsky A and Stebbins A 1997 *Phys. Rev. D* **55** 7368
- [23] Keating B *et al* 1998 *Astrophys. J.* **495** 580
- [24] Zhang Y, Hao H and Zhao W 2005 *Acta. Astron. Sin.* **46** 1
- [25] Grishchuk L 2006 *Usp. Fiz. Nauk* **176** (*Preprint gr-qc/0504018*)
- [26] Riess A *et al* 1998 *Astrophys. J.* **116** 1009
- [27] Perlmutter S *et al* 1999 *Astrophys. J.* **517** 565
- [28] Bahcall N A, Ostriker J P, Perlmutter S and Steinhardt P J 1999 *Science* **284** 1481
- [29] Spergel D N *et al* 2003 *Astrophys. J. Suppl.* **148** 175
- [30] Zhang Y 2002 *Gen. Rel. Grav.* **34** 2155
Zhang Y 2003 *Gen. Rel. Grav.* **35** 689
- [31] Fbris J C, Goncalves S V B and Santos M S 2004 *Gen. Rel. Grav.* **36** 2559
- [32] Santos M S 2005 *Proc. Conf. on Magnetic Fields in the Universe: From Laboratories and Stars to Primordial Structures* ed E M de Gouveia Dal Pino, G Lugones and A Lazarian (New York: AIP) (*Preprint gr-qc/0504032*)
- [33] Zhang Y *et al* 2005 *Class. Quantum Grav.* **22** 1383
- [34] Zhang Y and Zhao W 2005 *Chin. Phys. Lett.* **22** 1817
- [35] Grishchuk L 1974 *Sov. Phys. JETP* **40** 409
- [36] Zel'dovich Ya B and Novikov I D 1983 *The Structure and Evolution of the Universe* vol 2 (Chicago, IL: University of Chicago Press)
- [37] Parker L 1969 *Phys. Rev.* **183** 1057
- [38] Peiris H V *et al* 2003 *Astrophys. J. Suppl.* **148** 213
- [39] Seljak U *et al* 2005 *Phys. Rev. D* **71** 103515
- [40] Parker L 1979 The production of elementary particles by strong gravitational fields *Asymptotic Structure of Space-Time* ed S Deser and M Levy (New York: Plenum)
- [41] Bunch N D and Davies P C W 1982 *Quantum Fields in Curved Space* (Cambridge: Cambridge University Press)
- [42] The LISA sensitivity curve can be obtained from <http://www.srl.caltech.edu/shane/sensitivity/>
- [43] Maggiore M 2000 *Phys. Rep.* **331** 283
- [44] Maia M R G 1993 *Phys. Rev. D* **48** 647